Multi-Voltage Level Active Distribution Network with Large Share of Weather-Dependent Generation

Aeishwarya Baviskar, *Student Member, IEEE,* Kaushik Das, *Senior Member, IEEE,*
Matti Koivisto, *Member, IEEE,* and Anca Daniela Hansen, *Member, IEEE*

***Abstract*—This paper presents a comprehensive multi-voltage level active distribution network model based on real network data along with load and generation time-series for over a year. The network topology is based on a real distribution network in Denmark. The distribution network is embodied with a large share of renewable generation sources, with generation time-series simulated from meteorological data. In recent years, installations of wind power and photovoltaics along with behind the meter storage and electric vehicle charging stations have increased at the medium and lower voltage levels. These distributed generators and modern network assets are gaining traction due to the global climate change policies and local government initiatives to support low-carbon technologies in the grid. Utility operated small scale wind and solar power plants along with consumer end roof-top solar photovoltaic installations are expected to be increasingly connected to distribution networks at lower voltage levels. This situation requires a better understanding of the impact of high penetration of weather-dependent renewable energy sources on the operating conditions of the distribution network at both medium and low voltage levels. Despite the need, however, a multi-voltage level distribution network model has not been presented for power system simulation studies based on real network and weather-dependent renewable energy generation data.**

***Index Terms*—active distribution network, weather-dependent generation, time-series, optimization, dynamic time-warping.**

I. Introduction

ACTION against climate change has pushed forward technological advances in sustainable and carbon-neutral solutions in all fields of life, encompassing power generation. The past decade has already seen a massive movement towards renewable energy sources such as wind and solar energy installations [1]–[3]. The installed wind power capacity in Europe achieved a new peak in 2019 at 205 GW [2]. Countries like Denmark and Scotland with extensive wind resources have, in the recent years, met 47% (2019) and 97% (2020) of their electricity demands through Renewable Energy Sources (RES) especially wind energy. Half of Denmark's wind power capacity, about 3 GW, and about 70% of Scotland's total RES power capacity is based on onshore wind power. An increasing amount of RES, such as distributed wind turbines or small scale concentrated Wind Power Plant (WPP)s and Photovoltaic (PV)s plants, are also being connected to the lower voltage levels of the distribution networks. Furthermore, storage units, electric vehicle (EV) charging stations, combined heat power plants are gaining increasing popularity, and have a potential to become an integral part of the future distribution grid. Thus, a future distribution network no longer resembles a passive network with uni-directional flow of energy which creates new and unfamiliar challenges for the Distribution System Operator (DSO)s.

The main hurdle behind cost effective operation of distribution network with large share of weather-dependent RES is due to their intermittent/fluctuating and non-dispatchable nature as discussed in [4]–[6]. However, power electronics present in RES such as PVs and WPPs, electricity storage units, EV charging stations, imparts these installation with advanced control capabilities which convert them into active network assets. It is thus necessary to study, analyze, and develop active management techniques for the growing number of beneficial network assets connected in the distribution grid. For this purpose a benchmark distribution network model is required which incorporates a large share of RES and other network assets. Additionally, these assets are connected at different voltage levels (owing to power carrying capabilities of different voltage levels). For example, in distribution networks some of WPPs are connected at 60 kV network, while the roof-top PVs are connected at 400 V networks. When the assets are controlled in each of these different voltage levels, the change in power flows not only impact that specific voltage level but also other voltage levels too in terms of voltage profile, power losses, reactive power flow etc. This has further impact on the reactive power flow to the transmission network. As a result, a benchmark distribution network model representing the characteristics of large share of integrated generations in each voltage level is of particular interest.

The design of benchmark models in power systems has been a topic of interest for many research works. The benchmark models presented by the CIGRE Task force are one the most commonly used and well known distribution network benchmark models. The CIGRE Task Force developed distinct high, medium and low voltage benchmark networks for studying and analyzing network behavior in presence of Distributed Energy Resource (DER) and RES [7]–[9]. Another set of benchmark models that demand noteworthy attention are the network models presented by the IEEE Task Force. However, the IEEE benchmark models are designed to be used for small-signal studies in the power systems and not for analyzing impact of RES in the distribution network operation [10]. *SciGRID* is also an example of open source network model intended towards studying congestion management, transmission ca-

Aeishwarya Baviskar, Kaushik Das, Matti Koivisto, and Anca Hansen are with Technical University of Denmark

This project has received funding from the European Union's Horizon 2020 research and innovation program under the Marie Sklodowska-Curie grant agreement No 861398.

Manuscript received March , 2021; revised August 26, 2015.

pacity, grid stability in the transmission networks developed on data from *Open Street Maps* [11], [12]. Furthermore, to address the overestimates of grid extension needed due to increasing DER and storage installations in transmission and distribution networks, a synthetic open-source medium voltage distribution network, called the *eGo grid model*, is presented in [13]. The *eGo grid model* is designed using an open source software called the DIstribution Network GeneratOR (DINGO) for generating synthetic networks, emphasizing the growing interest in analyzing distribution network behavior pertaining to the aforementioned developments. To enhance understanding of network behavior and characteristics, and needs of future distribution networks with RES and other low-carbon technologies, [14] establishes *Low Voltage Network Models and Low Carbon Technology Profiles* founded on the UK distribution network. Examples of works addressing generation of benchmark models can be found in [15], [16]. *SimBench* is one of the more recent additions to the library of open-source benchmark models developed on principles presented in [16], [17]. The grid data in *SimBench* is in accordance with the German DSO's operation and planning principle. Furthermore, *SimBench* also provides load time-series for about one year for different types of consumer behavior. Sarstedt et. al. [18] present an integrated transmission and distribution network model, wherein the topology for the lower voltage networks is synthetically generated. More often the network topology deployed in the present open-source models is based on synthetic network modeling. Furthermore, amongst all the distribution network models presented so far, there are only two multi-voltage network models which include the low voltage levels [17], [18].

In spite of the already many existing benchmark models in the literature so far, there is a lack in a comprehensive multi-voltage level active-distribution network model, based on real network topology, incorporating a very high share of weather dependent RES, with load and generation time-series for a long duration covering different weather and load conditions. In this respect, this article proposes and presents such a multi-voltage level distribution network model, which is needed for an exhaustive study of the performance, operation and control of future weather-dependent distribution networks in terms of grid requirements and specifications, flexibility requirements for future RES technologies, as well as in developing advanced control strategies to improve the overall operating conditions of such distribution networks.

The proposed benchmark distribution network model, entitled as the *DTU 7k Bus Active Distribution Network*, is an open-source and it can be used in analyzing distribution networks with large share of distributed generation such as RES, combined heat and power plants, storage, wide spread use of electric vehicles, etc. Furthermore, it has the flexibility to incorporate additional network assests to investigate performance of active distribution network. Additional applications for the *DTU 7k Bus Active Distribution network* can also be found in development of control and optimization algorithms for active management of future distribution network with aforementioned assets. The network has, at its foundations, data from a real 60 kV distribution network topology along with measurement data for load time-series and wind power generation. Hence, a top down approach is applied in its development.

The main important novel features of the proposed and developed benchmark distribution network model are as following:

- Network topology is modeled from geographical layout of consumer supply points
- 18 different topologies of 10 kV-400 V networks with different characteristic loads and RES
- Large share of embodied weather-dependent generation, PV and WPPs
- Weather-dependent generation time-series simulated from meteorological data
- Load time-series derived from measurement data
- Flexibility to incorporate additional network assets such as combined heat and power plants, storage units, electric vehicle charging stations, etc.
- Comprehensive platform for development of coordinated control between different assets for optimal operation of distribution network, while incorporating uncertainty from weather dependent generation and loads.

Section II briefly introduces the *DTU 7k Bus Active Distribution Network* along with the publicly available data for the network. The raw data used to develop the distribution network model and methodology is described in Section III. Section IV and Section V shed light upon the results of the implemented methodology and present a discussion giving an insight into the *DTU 7k Bus Active Distribution Network* and its future applicability respectively.

II. DTU 7k-Bus Active Distribution Network

The DTU 7k-Bus Active Distribution Network is a multi-voltage network with a high share of weather-dependent renewable energy generation. It spans across 3 voltage levels, namely 60 kV, 10 kV and 0.4 kV while being connected to the transmission grid via a step-up 60 kV/150 kV transformer at the 0^{th} Bus which serves as the slack bus for the entire system. This section presents key features of the DTU 7k Bus Active Distribution Network.

A. The 60 kV Network

The medium voltage (MV) 60 kV network consists of 25 buses out of which 23 buses are connected to 60 kV/10 kV substations. The 60kV/10kV substations are equipped with on-load tap changing (OLTC) transformers. A cumulative wind generation capacity of 45 MW is connected at three different nodes in the MV network at 60kV. It is important to mention that the network topology for the MV network originates from a real Danish distribution network. Table I lists key elements of the Medium Voltage (MV) network and Fig. 1 illustrates the network topology.

The maximum power flow from the 150 kV transmission network to the MV network is $\approx$ 60 MW while the reverse power flow from the MV network to the transmission network is at a maximum of 150MW, which is more than the total installed wind in the 60 kV network, based on historical

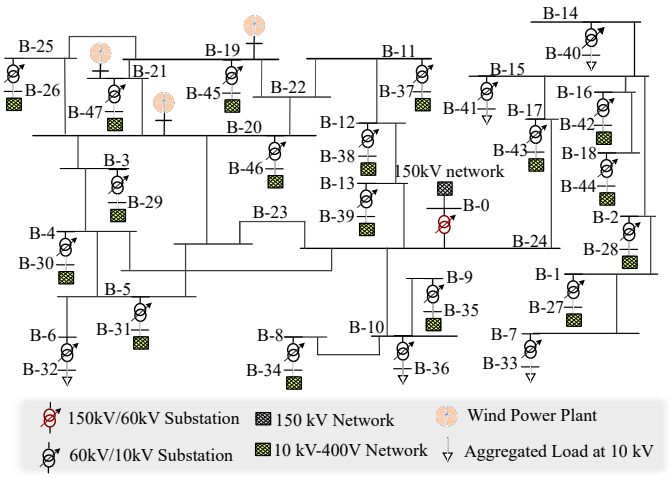

Fig. 1: 60kV Network

data of 1 year. At the 60kV/10kV substations, 17 of the 23 substations record negative power flows; confirming the presence of generating sources in the 10 kV-0.4 kV network. Time-series data of load, aggregated at 10kV and generation profiles for the 3 WPPs, derived from measurement data in the network, forms the basis for the development of the presented multi-voltage network.

TABLE I: The 60kV distribution network

Network Element	#	Voltage Level
Buses	24	60 kV
	23	10 kV
HV/MV substation	1	150 kV / 60 kV
MV/LV substation	23	60 kV / 10 kV
MV/LV substation with controllable generation	3	60 kV / 10 kV
Type IV controllable WPPs	3	60 kV
Aggregated Loads	6	10 kV
Expanded LV networks	17	10 kV-400 V

B. 10 kV-0.4 kV Networks

The 10 kV-0.4 kV networks connected at 17 different 10 kV nodes from the 60 kV network extend the principal network to build the multi-voltage network. A total of 6541 nodes at 0.4 kV and XXX nodes at 10 kV nodes are distributed across the 10 kV-0.4 kV networks. The networks also accommodate 291 10 kV-0.4 kV substations with off-load tap changing transformers. In addition, the 10 kV-0.4 kV networks have 107 MW of wind and 25 MW of PV installed capacity. A breakdown of the number of 10 kV-0.4 kV substations, consumer nodes, wind and PV capacities per 10 kV-0.4 kV network is provided in Table II. Table II also lists the aggregate demand of 4 kinds of Standard Load Profile (SLP)s available. It is important to mention that the 10 kV-0.4 kV network load profiles are formulated from 27 different SLPs provided by *SimBench* which categorizes the SLPs into household, agricultural, commercial, and miscellaneous profiles as shown in Fig. 4. The aggregate amount of household, agricultural and commercial load demand from the 10 kV-0.4 kV networks is 27.9 MW, 18.5 MW and 30.5 MW respectively. The proportion

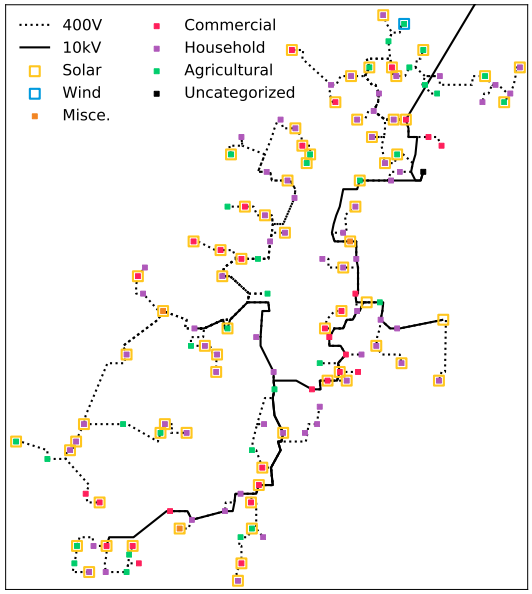

Fig. 2: 10 kV-400 V Network at Bus 27

of household, agricultural and commercial SLPs in the Low Voltage (LV) network, which is determined based on the time-series data derived from measurement data, varies for each LV network. The composition of different categories of SLPs in the 10 kV-0.4 kV network gives a further insight into the loads connected at the network. For example, since Bus 46 contains no share of agricultural load profiles, the 10 kV-0.4 kV network at Bus 46 can be assumed to be a snap-shot of an urban residential area. Similarly, it can be said that the 10 kV-0.4 kV network at Bus 43 is a industrial area due to large share of commercial load profiles as compared to household and agricultural loads.

Fig. 2 and Fig. 3 show the network topology for the LV networks at buses 27 and 46 respectively. These two buses are chosen for depiction because LV network connected to Bus 27 has one of the least, while LV network at Bus 46 has the highest number of 400 V and 10 kV nodes. As illustrated in Fig 2 and Fig. 3 the aggregated household, agricultural and commercial loads along with weather-dependent generation is distributed amongst the 400 V and 10 kV nodes. Differentiation of SLPs at different nodes is not indicated in Fig. 2 and 3 due to space constraints. The prosumer nodes in networks 27 and 46 are indicated with an orange or blue box around the load profile, if applicable, indicating a PV or WPP installation at that node. In network 46, $\approx 44.7\%$ nodes are connected to a weather-dependent generation, whereas, in network 27, $\approx 52\%$ nodes are connected to weather-dependent generating sources.

C. Weather-Dependent Generation

The multi-voltage network presented in this research is developed with the objective of studying the effect of the stochastic nature of weather-dependent generation connected at the medium and lower voltage networks. The proposed

TABLE II: Key features of 10 kV-400 V distribution networks

Bus #	Substation 10 kV / 400 V	Nodes 10 kV	Nodes 400 V	Generation [MW] PV	Generation [MW] WPP	Loads [MW] Household	Loads [MW] Agricultural	Loads [MW] Commercial	Loads [MW] Miscellaneous
26	18	1	329	0.73	0	1.3	1.05	1.3	0.12
27	5	3	134	1.85	0.44	1.95	1.75	1.82	0.16
28	10	1	270	0.57	0	0.52	1.35	1.85	0.10
29	21	1	397	1.42	7.66	1.3	0.71	1.18	0.11
30	17	1	440	1.21	11	2.6	1.58	2.56	0.59
31	15	1	390	1.93	3.34	2.3	1.15	1.42	0.12
34	1	1	387	1.3	2.61	1.16	1.3	1.8	0.14
35	24	1	32	1.66	9.25	1.27	1.83	1.48	0.10
37	22	1	516	1.65	9.61	0.82	0.63	1.73	0.20
38	17	1	477	1.27	5.56	1.42	1	1.6	0.26
39	21	1	408	3.2	8.83	3.54	1.80	1.86	0.08
42	24	1	493	2.32	6.2	2.56	0.12	0.65	0.38
43	16	1	618	0.61	0.32	1.47	1.98	**5**	0.55
44	21	1	456	0	0	0.56	0.63	1.28	0.08
45	21	1	440	2.1	12.66	1.52	1.08	2.077	0.41
46	**17**	**9**	**494**	**3.37**	**21.44**	**2.75**	**0**	**1.88**	**0.30**
47	18	1	260	0.45	9	0.88	0.474	0.96	0.08
$\sum$	**291**	**17**	**6541**	**25.56**	**107.87**	**27.9**	**18.5**	**30**.5	**3.8**

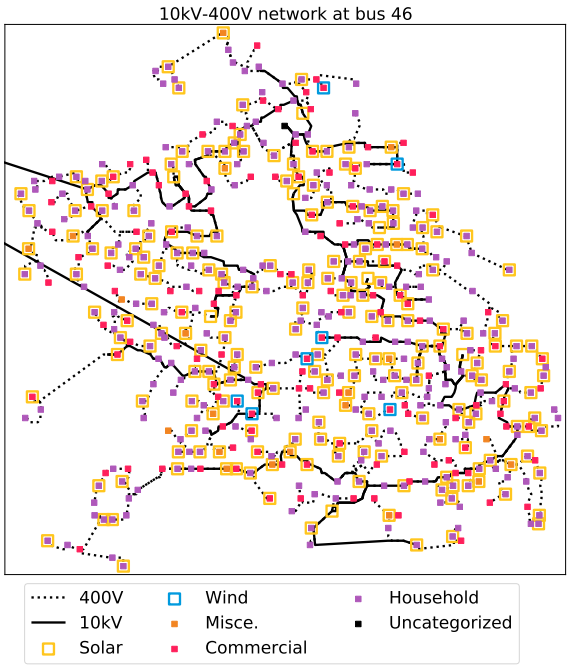

Fig. 3: 10 kV-400 V Network at Bus 46

multi-voltage network has a high volume of installed weather-dependent generation in the form of wind and PV.

From Table II, it should be noticed that 9 out of 17 10 kV-0.4 kV networks have a WPP generation capacity of more than 5 MW and only one 10 kV-0.4 kV network, at Bus 44, is devoid of any generation capacity. The 10 kV-0.4 kV networks connected to buses 45, 46 and 47 have high volume of WPP generation capacities. In addition, the three 10 kV buses i.e. 45, 46, 47, are also connect to WPPs on the 60 kV side of the substation. Amongst which Bus 46 is connected to one of the largest LV distribution networks with 494 number of 0.4 kV nodes, 21.44 MW of installed WPPs and 3.37 MW of installed PV capacity. Whereas Bus 20, connected to Bus 46 with a step down transformer, also has an WPP with installed capacity of 15 MW, which together accounts approximately 39 MW of weather-dependent generation at a single node.

It should also be mentioned that all WPPs in the 10 kV-0.4 kV network have a capacity of 300kW and above, being connected to 10 kV nodes. In contrast to WPP, the PV generators are connected to both 10 kV and 400 V nodes. This makes part of the 400 V nodes prosumers. The term prosumer means that these nodes both produce as well as consume electricity.

D. Possible Applications

The shift in the role of distribution system from a passive entity to an active entity is the primary impetus behind this research. Since the distribution network model presented in this research is derived majorly from actual network data, it serves uniquely as a benchmark model to study the effects of various weather-dependent energy sources along with storage, EV and other modern applications in the distribution grid. Some of the possible areas of application are as follows,

- Investigate impact of a large share of weather-dependent RES on distribution network operations
- Develop advanced control strategies to improve the operating conditions of an Active Distribution Network with a large share of RES
- Analyze performance of network assets, such as on-load tap changers, voltage regulators, switching capacitors and reactors, supporting the distribution grid operation
- Quantify the flexibility requirements for future RES technologies
- Design active control for hybrid power plants in the active distribution network
- Evaluate impact of altered distribution network characteristics on the TSO/DSO interface
- Explore co-ordination opportunities between transmission and distribution network, re-introducing distribution network as an active asset to the transmission network
- Assess the impact of limited observability of RES connected at the consumer end
- Inspect opportunities arising from negatively correlated generation sources such as PVs and WPPs

E. How to access the data?

The distribution network described in this section is an open-source dataset and available in an online repository *ADD DATA REPO*. The dataset in the repository is the first version of the DTU 7k-Bus Active Distribution Network and is expected to undergo modifications as the work progresses.

All the network files in the dataset are *csv* files suitable to be directly used in MatPower, PandaPower or Pypower. Further description of the data can be found in the readme file included.

III. Network Modeling Methodology

This section briefly describes the methodology used to generate the DTU 7k Active Distribution Network. First, an insight is provided into the raw data used to generate the network. After that, an optimization algorithm to estimate the share of various standard load profiles and weather-dependent renewable energy sources is outlined. The heuristics based on statistical information about 10kV networks deployed for the profile assignment to each 400V node are then elaborated.

A. Raw Data

60 kV Network: The network topology, line and transformer data for the 60 kV network are based on a real Danish distribution network. The aggregated load time-series at 10 kV and the WPP generation data are measurement data provided by Eniig Forsyning A/S [19]. This data forms the basis on which the entire DTU 7k-Bus Active Distribution Network is developed.

10 kV Network Topology: The network topologies for all the LV networks are generated from an online tool, Distribution Network Models module (DiNeMo), provided by the European Commission, Joint Research Centre [20]. DiNeMo takes as input an area of interest from *Open Street Map* [12] and reproduces a representative distribution grid. The inputs to DiNeMo for generating LV networks in this work are based on an approximate geographical area for the location of the 60 kV / 10 kV substations indicated in Fig. 1. In addition to the geographical location of the distribution network DiNeMo also takes as input, population / consumer density, probability of consumers per building [%], Minimum LV demand [kW], Minimum MV demand [kW], Voltage level [kV], and transformer capacity for the location.

The National Denmark Statistics [21] provides references for inputs such as the population density and probability of consumers per building. The maximum demand for each node is determined based on the aggregated load profile at 10 kV provided by [19], hence, the minimum demand was set arbitarily to 10 kW while generating the LV networks in DiNeMo. It should be mentioned that the inputs the LV networks are derived from the Danish Statistics to generate network which are as realistic as possible in terms of energy consumption patterns in each network. Thus, even though the network topology and DiNeMo inputs originate primarily from Denmark, the DTU 7k-Bus Active Distribution Network serves as a generic distribution grid model consisting of LV networks with diverse consumption patterns as highlighted in Table II.

As outputs, DiNeMo also provides line, MV/LV substation data, switches in the network, and load data at each node. The line and MV/LV substation data is used directly and provided in the *MatPower* or *PyPower* format. The load data from DiNeMo lists a demand in *kVA* for each node based on the maximum demand input provided at the time of network generation. The demand in *kVA* provided by DiNeMo is then used to scale and assign SLPs at every node in the network.

Standard Load Profiles: The method used in this work to allocate share of specific load and generation profiles, is to decompose the aggregated load profile at 10 kV into various SLPs. The SLPs are provided by *SimBench*, which is an open-source database for power load, generation and storage time-series [22]. However, the generation time-series for WPPs and PVs used for developing the network model is based on meterological data, hence, only 27 load-time series for the LV networks provided in *SimBench* are used.

The SLPs are grouped into 4 categories such as household (H), agricultural (L), commercial (G) and miscellaneous (B). There are 15 commercial, 6 household, 4 agricultural and 2 miscellaneous SLP. The SLPs are also classified according to level of consumption into low, medium, and high as illustrated in Fig. 4.

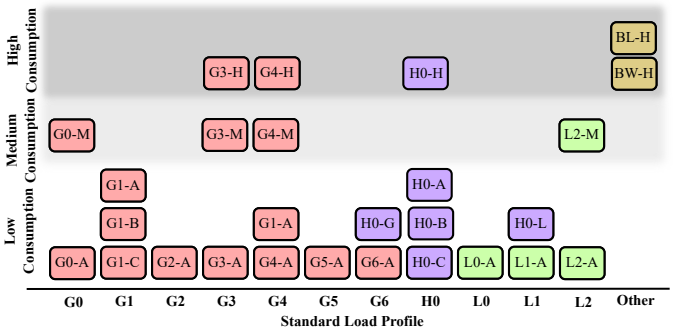

Fig. 4: Standard Load Profiles from SimBench

Wind and Photovoltaic generation profiles: All the wind power generation profiles and photovoltaic profiles provided with the data set are generated using DTU Correlations in Renewable Energy Sources (CorRES) simulation tool. The weather-dependent generation profiles are simulated using meteorological time-series and stochastic simulations [23].

For generating PV profiles, the input provided to CorRES is the geographical location of the PV plant, installed capacity [MW], surface azimuth angle and surface tilt. The location for the PV installation is approximately at at the center of the geographical area of the LV network whereas, the installed capacity is set to 1 MW for all the PV installations. By setting the installed capacity to 1 MW, the PV generation profile from CorRES can be used as a p.u. profile and scaled according to the installed capacity for each LV network. Since, the geographical span of any of the LV networks is constrained to a small area, only one PV profile is generated per LV network, i.e. there is one unique LV profile for every LV network. The Global Solar Atlas [24] provides optimal inputs for the surface azimuth angle and tilt for the chosen geographical location.

Similar to PV installations, the geographical locations for WPP installations are assumed closer to the 60 kV / 10 kV substation. The data register for wind power plants provides a comprehensive list of WPP installations across Denmark [25]. Thus, WPP installations closer to the 60 kV /10 kV substation are chosen for simulation and generating wind power profile for each LV network. Consequently, there are multiple WPP generation profiles for some of the LV networks. In contrast to PV profiles, simulating WPP profiles from CorRES requires a number of inputs, such as, the hub height, installed capacity, number of turbines, turbine rated power, turbine diameter, etc. All of the input data for simulating WPP profiles is taken from the data register of wind power plants, and thus represents real WPP installations at the location of the LV network.

B. Optimization Algorithm

The goal of the optimization is to decompose/categorize an aggregated load time-series into SLPs and weather-dependent generation profiles (PV and Wind) as shown in Fig. 5. The basis of this decomposition is the aggregated load time-series at 10 kV or at the LV side of the 60 kV/10 kV substations in the 60 kV network. *SimBench* SLPs and weather-dependent generation profiles obtained from CorRES are assumed constant and known during the optimization. The optimization then defines the share of each SLP and weather-dependent generation profile for one particular LV network. Thus the output of the optimization for the SLPs is the aggregate demand of each SLP in the LV network, while for the weather-dependent generation is the aggregate generation from each generation profile. The uncategorized profile in Fig. 5 refers to the part/behavior of the aggregated 10 kV profile which could not be captured using the given SLPs and weather-dependent generations.

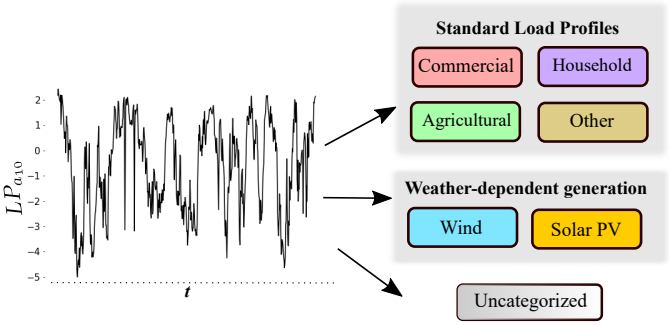

Fig. 5: Decomposition of Load Profile

To formulate an optimization problem to determine the cumulative maximum demand and generation in an LV network, the following notations are defined,

- P_t: aggregated load at 10 kV at time t in MW
- $\mathcal{S}$: set of all SLPs from *SimBench*
- $l_{i,t}$: power demand for the i^{th} SLP at time t in p.u., $i \in \mathcal{S}$
- d_i: aggregated demand from the i^{th} SLP in MW, $i \in \mathcal{S}$
- $\mathcal{R}$: set of all generation profiles from CorRES
- $w_{j,t}$: power generated from the j^{th} weather-dependent generation profile at time t in p.u., $j \in \mathcal{R}$
- g_j: aggregated generation from the j^{th} generation profile in MW, $j \in \mathcal{R}$

It is assumed that the d_i and g_j reflect additive effect of several nodes and weather-dependent generation installations in the LV network. Hence, it is often called the aggregate value for an LV network. Let $\mathbf{L}_t$ be the vector of load demands in p.u. for all SLPs at time t,

$$\mathbf{L}_t = \begin{bmatrix} l_{1,t} & l_{2,t} & \dots & l_{27,t} \end{bmatrix} \tag{1}$$

whereas, $\mathbf{W}_t$ is the vector of generation for each solar and wind profiles in p.u. at time t,

$$\mathbf{W}_t = \begin{bmatrix} w_{1,t} & w_{2,t} & \dots & w_{k,t} \end{bmatrix} \tag{2}$$

Note that there is only one PV profile per LV network. Therefore, $pg_{1,t}$ is the per unit value of solar generation in the network. As mentioned earlier, it is possible to have multiple WPP profiles for one LV network referring to [25]. It is thus assumed that there are $k-1$ WPP profiles available, which implies that,

$$w_{j,t} \dots \forall j \geq 2 \tag{3}$$

denotes the WPP generation at time t in per unit.

Let $\mathbf{D}$ be the vector with cumulative maximum demand for all SLPs,

$$\mathbf{D} = \begin{bmatrix} d_1 & d_2 & \dots & d_{27} \end{bmatrix} \tag{4}$$

and vector $\mathbf{G}$ contains the maximum weather-dependent generation for solar and wind profiles,

$$\mathbf{G} = \begin{bmatrix} g_1 & g_2 & \dots & g_{k,a} \end{bmatrix} \tag{5}$$

Let ε_t denote the difference between aggregated load at 10 kV and SLPs along with weather-dependent generation, at time t, namely uncategorized load profile. This is given by the following equation,

$$\varepsilon_t = P_t - \mathbf{L}_t \mathbf{D}^T + \mathbf{W}_t \mathbf{G}^T \tag{6}$$

The objective function for the optimization is to reduce the root-mean square error of ε_t, e.g.:

$$\min_{\mathbf{D},\mathbf{G}} \sqrt{\frac{1}{T_f} \sum_{t=1}^{T_f} \varepsilon_t^2} \tag{7}$$

where T_f is the length of the available time-series. The output of the optimization is aggregate demand for all SLPs, $\mathbf{D}$, and aggregate solar and wind power generation, $\mathbf{G}$, for any LV network. The control variables for the optimization problem are unconstrained and unbounded. Furthermore, the equations stated above indicate a non-linear optimization problem which is solved in *Python* using *CPLEX*.

Dynamic Time Warping: One of the earliest works in Dynamic Time Warping (DTW) is in the area of speech recognition [26], [27]. Authors in [26] introduce DTW as a pattern matching algorithm wherein the time-axis fluctuation is modeled with a nonlinear warping function. The time-warping function is then applied to eliminate time differences between two signals for maximum coincidence. The problem is drafted as an optimization problem, or more specifically a dynamic

programming problem, with the time-warping function being the optimization variable [26], [28], [29]. The *dtw* package in *Python* is used to implement DTW algorithm on the available time-series.

DTW is used to match the aggregated 10 kV load time-series and the solution obtained via the optimization problem in Equation. (7). This step reduces temporal mismatch between the SLPs and the aggregated load time-series at 10 kV. The *dtw* function generates a time warping vector $\mathbf{F}_t$ given the reference time-series and the preliminary solution time-series obtained after optimization.

$$\mathbf{F}_t = dtw(P_t,\ \mathbf{L}_t\mathbf{D}^T - \mathbf{W}_t\mathbf{G}^T) \tag{8}$$

The time-warping vector is then used to warp $\mathbf{L}_t$ only, since the weather-dependent generation depends on meteorological data at the same geographical location as the LV network. Hence, the solution time-series after DTW is given by the expression,

$$\mathbf{L}_t(\mathbf{F_t})\mathbf{D}^T - \mathbf{W}_t\mathbf{G}^T \tag{9}$$

C. Profile assignment

After obtaining the aggregate load demand for each SLP for an LV network, the next step is to assign every node in the LV network obtained from DiNeMo with a unique SLP and installed capacity.

DiNeMo generates a consumer data statistics highlighting maximum demand, termed *Dem_kVA*, at each node, along with the network topology. The *Dem_kVA* value at any node is an integer multiple of the minimum *kVA* demand input provided while generating the distribution network in DiNeMo. Assume that the minimum demand in the LV network at any node is s_{min} and that there are N nodes (400 V and/or 10 kV) in the LV network. Thus, load demand for any n^{th} node in the network provided by DiNeMo is given by,

$$x_n = h_n s_{min} \tag{10}$$

where h is an integer within minimum and maximum bounds of 0 and h_{max}.

The total maximum simultaneous demand, according to DiNeMo, for the LV network, with N nodes, is thus,

$$X = \sum_{n=1}^{N} x_n = s_{min} \sum_{n=i}^{N} h_n \tag{11}$$

The results from the optimization suggest that the total maximum simultaneous demand for the LV network is sum of installed capacities for all the SLPs, termed Y, as follows:

$$Y = \sum_{i=1}^{27} d_i \tag{12}$$

The goal of designing a profile assignment algorithm is to assign every node in the LV network, with an unique SLP with capacity y_n such that y_n can be denoted by an integer multiple of s'_{min},

$$y_n = h_n s'_{min} \quad h_n \in 0, h_{max} \tag{13}$$

where s'_{min} is the scaled minimum demand for the LV network also satisfying the following equation,

$$Y = s'_{min} \sum_{n=1}^{N} h_n \tag{14}$$

Thus, s'_{min} can be calculated as follows,

$$s'_{min} = s_{min} \frac{Y}{X} \tag{15}$$

Subsequently assume that the aggregated demand for the i^{th} SLP, denoted by d_i, is equally distributed amongst k_i nodes, which implies,

$$d_i = t_i s'_{min} k_i \tag{16}$$

where, t_i is an integer multiple assigned for i^{th} SLP. Therefore k_i can be calculated as follows,

$$k_i = round(\frac{d_i}{t_i s'_{min}}) \tag{17}$$

Note that the RHS in Eq. (17) is rounded off to the nearest integer since the number of nodes with i^{th} SLP must be an integer. Notice that there are still two unknowns in the above equation namely, t_i and k_i. A heuristics based approximation is used to determine the value of t_i for the network supported statistical data from SimBench. SimBench classifies all the SLPs into broadly 3 level of consumption categories, low, medium, and high, as shown in Fig. 4. Let, s_i, denote the power demand for any SLP of class i assigned to one node. This imposes an additional condition on demand for each profile which will aid is assignment of the standard load profiles to the nodes. The following thus makes the foundation of the heuristic approximation,

$$s_H \geq s_M \geq s_L \geq s_G \geq s_C \geq s_B \geq s_A \tag{18}$$

where $H, M, L, G, C, B,$ and A are the SLP categories as indicated in Fig. 4. Note that Eq. (18) is not implemented as a hard constraint. Thus, from Eq. (16) and Eq. (18) the following condition can be accepted for the order of t_i,

$$t_H \geq t_M \geq t_L \geq t_G \geq t_C \geq t_B \geq t_A \tag{19}$$

while,

$$t_i \in [1, h_{max}] \tag{20}$$

The above stated problem is solved heuristically. The principal idea is to begin profile assignment from the nodes with maximum demand, Dem_kVA value, according to DiNeMo and allocate number of nodes for each SLP in the network, i.e. k_i, corresponding with cumulative capacity for each SLP d_i and an appropriate multiplying factor t_i. The heuristic profile allocation algorithm assigns a single SLP to each node, hence,

$$N = \sum_{i=1}^{27} k_i \tag{21}$$

Let, $\mathbf{K}$ be the vector with the number of nodes assigned to each SLP,

$$\mathbf{K} = \begin{bmatrix} k_1 & k_2 \dots k_{27} \end{bmatrix} \tag{22}$$

The maximum demand for the SLPs is thus given by the following element-wise division,

$$s_i = d_i/k_i \ldots \forall i \in [1, 27] \tag{23}$$

Finally, the maximum demands at each node along with the corresponding SLP are assigned to the nodes in the 10kV-400V network, starting from the $max(\mathbf{S})$ in a descending order of maximum demands at nodes given by DiNeMo.

In addition to load profiles, the aggregated PV and WPP generation capacities are assigned to appropriate nodes in the network. The following assumptions are considered while allocating the weather-dependent generation in any LV network:

- Minimum installed PV capacity: 1 kW
- PV generation can be installed at 400 V or 10 kV nodes
- Minimum installed WPP capacity: 300 kW
- WPPs are installed only at 10 kV
- Installed generation at any consumer node is less than its maximum demand

Statistics for solar installations in the Danish grid, provided in [1], show that the self-consumption via PV generation is in the range of 20-30% for the residential sector and about 40% for the commercial sector, for the years in question. Residential PV plants, i.e. rooftop plants, have an installed capacity of 7 kW or less, in particular 3 kW PV installations being greatly preferred, while for the commercial sector PV installed PV capacity is 7 kW or higher. Taking into account the statistics described in [1], the aggregated PV capacity for an LV network is assumed to supply 25% of the simultaneous maximum demand for household SLPs and 40% of the simultaneous maximum demand for commercial and agricultural SLPs combined. Note that the simultaneous maximum demand for the household SLPs is sum of the aggregated demands (d_i), calculated by the optimization, for all the household SLPs (HX-X).

In order to assign WPPs at the 10 kV node, wind installation statistics from [25] are used as a reference. For the geographical area of the LV networks, the maximum onshore wind installation is in the range of 3.6 MW-4 MW. However, a large number of WPPs have installed capacities of 1 MW. Note that, the number of 10 kV nodes in the network is significantly less than the number of 400 V nodes. Hence, for assigning WPPs to the 10 kV nodes, a maximum to minimum approach is adopted. This implies that the aggregated wind power generation is divided into groups of 3.6 MW WPPs and a remainder value if applicable. If the aggregated wind power generation for an LV network is less than 3.6 MW, the entire aggregated wind power generation is assigned to one single 10 kV node. Exception to this is the LV network at Bus-35, which accommodates only one 10 kV node. Thus, this 10 kV node in the LV network at Bus-35 is connected to a WPP with installed capacity of 9.25 MW.

IV. Results

The optimization results are depicted and described for LV network at bus 27 which serves as representative network for all the LV networks. A power flow analysis is also performed for this network.

A. Optimization for network modeling

The optimization algorithm described in the previous section is designed with an intention to categorize, to a maximum amount, the aggregated load profile at 10 kV into available SLPs and weather-dependent generation profiles. In principal, the aggregated load profile at 10 kV is expected to be represented by a sum of varying proportions of theSLPs and weather-dependent generation. Thus, the objective function for the optimization is designed to represent and minimize the mismatch between the aggregated load profile at 10 kV and cumulative sum of the SLPs and weather-dependent generation, by a root mean square value.

The first step in the optimization methodology is to obtain a preliminary solution of the optimization problem given in Equation (7). The solution of the optimization problem without DTW is given by the following expression and will henceforth be referred to as the preliminary solution,

$$\mathbf{L}_t\mathbf{D}^T - \mathbf{W}_t\mathbf{G}^T \tag{24}$$

The root mean square error for the preliminary solution is 0.31 MW. It is important to mention that, the maximum active power demand at bus no. 27 is 3.51 MW and the minimum active power demand is 0.26 MW. Thus, the root mean square error is $\approx 8.8\%$ of the maximum load at bus no. 27.

The next step is to perform DTW on the preliminary solution. For DTW, the aggregated load profile at 10 kV serves as the reference time-series and the preliminary solution as the target. A time-warping vector is calculated to align the preliminary solution to reference time-series. DTW is performed using the *dtw* package in *Python*. The root mean square error between the solution time-series after DTW is 0.28 MW, $\approx 8.1\%$ of the maximum load at bus no. 27. Thus, DTW reduces the root mean square between the reference time-series and the solution.

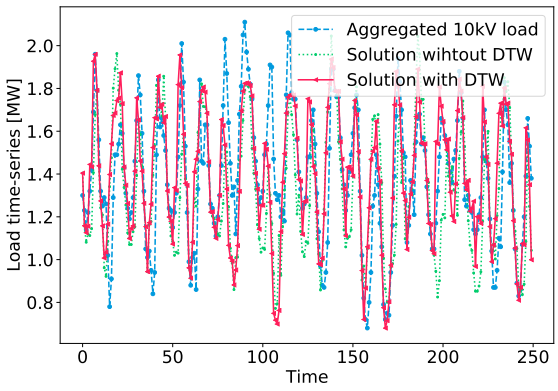

Fig. 6: Reference and solution time-series for 250 time-steps

Fig. 6 shows a snapshot of the aggregated 10 kV time-series, preliminary solution, and the final solution with DTW for 250 time-steps. It is observed from Fig. 6 that, neither the solution time-series after DTW nor the preliminary solution replicate the reference time-series entirely. This implies that available SLPs and weather-dependent generation profiles fail to completely categorize the characteristic behavior of the reference time-series. The difference between the solution with DTW

and the reference time-series is the un-categorized portion of the reference time-series. Note that the un-categorized time-series may or may not represent a load-only profile. Hence, it can be further categorized using a different set of SLPs representing variety of load/generation profiles such as electric vehicles, storage units, combined-heat cycle plants, etc.

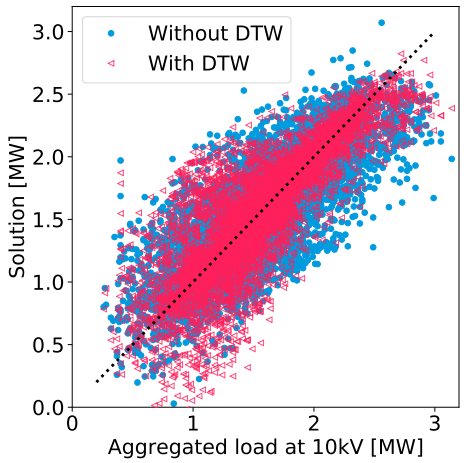

Fig. 7: Scatter plot for the solution time-series with and without DTW with respect to reference time-series

Another measure used to analyze the quality of the solution is the correlation between the reference and the solution time-series. Fig. 7 exhibits a scatter plot of the two solution profiles on the y-axis, i.e. with and without DTW, against the reference time-series on the x-axis. The scatter plot suggests that the solution profile with DTW is better aligned with the reference time-series in comparison to the preliminary solution without DTW. This is also evident from the fact that the correlation of the preliminary solution without DTW with the aggregate load profile is 0.78. DTW improves the correlation between the reference time-series and the solution time-series to 0.83.

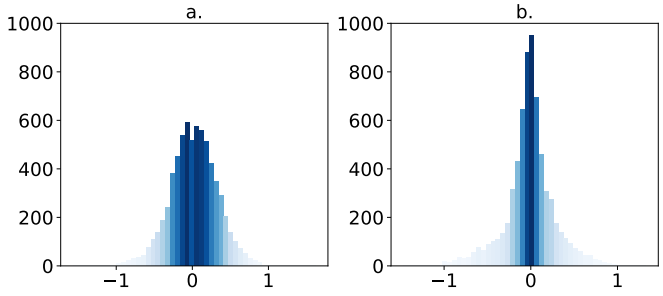

Fig. 8: **a.** Probability distribution for solution without DTW; **b.** Probability distribution for solution with DTW

The positive effect of performing DTW on the preliminary solution is most noticeable on the un-categorized time-series. Fig. 8 captures the probability distribution of the preliminary solution without DTW and the solution with DTW. After DTW the solution profile is more concentrated around *0* value compared to the preliminary solution without DTW. The 95^{th} percentile value for the probability distribution of the preliminary solution is 0.523 while the 95^{th} percentile for the probability distribution with DTW is 0.47 which further suggests a reduction in the mismatch between the reference and the solution.

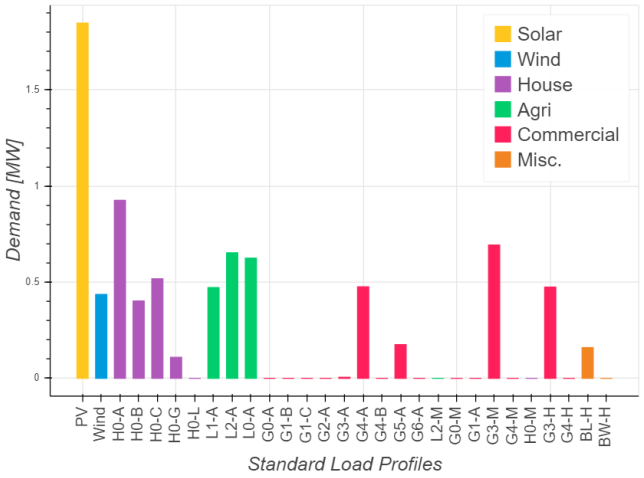

Fig. 9: Aggregate demand for SLPs and aggregated generation capacity for weather-dependent generation profiles

Fig. 9 shows the aggregate demands for all SLPs and aggregate generation for PV and WPP for LV network at Bus-27. Note that the PV generation in this network is $\approx$ 1.85 MW and wind generation is $\approx$ 0.44 MW. However, the maximum and minimum demand at Bus-27 is 3.51 MW and 0.26 MW. Thus, the weather-dependent generation in the LV grid was previously unobservable at the 60 kV/10 kV substation. Furthermore, aggregate share of household, agricultural and commercial loads in the network is 1.95 MW, 1.75 MW and 1.82 MW respectively. Population density of the geographical area for this LV network qualifies it to be a semi-urban/rural network. This justifies the presence of the agricultural load in an approximately equal proportion to commercial load. Also notice that, not all the SLPs have a non-zero aggregate load. Thus, the aggregated load time-series at 10 kV is not characterized by all of the SLPs.

The final step in generating the LV network, shown in Fig. 2, is to distribute all the SLPs amongst individual 400 V nodes using the heuristic algorithm described in Section III-C.

B. Power Flow

The result of the power flow calculation for one timestamp is provided in this section for the LV network at Bus-27. The power flow calculations are computed using Newton Rapson method in *PyPower*. Note that all the data-sets provided for the DTU 7k-Bus Active Distribution Network are in the format which can directly be used via *PyPower*, *MatPower* or *PandaPower* libraries.

A random timestamp is chosen to perform power flow calculations to establish the plausibility of the load and generation time-series along with the LV networks. All the 10 kV/400 V transformers are assumed to be equipped with off-load tap-changers and 60 kV/10 kV transformers are equipped with on-load tap-changers. Note that all the tap-settings in the network are set to the nominal position during the power flow

calculations. Fig. 10 depicts the voltages at all the nodes in the LV network for this timestamp. The load demand from

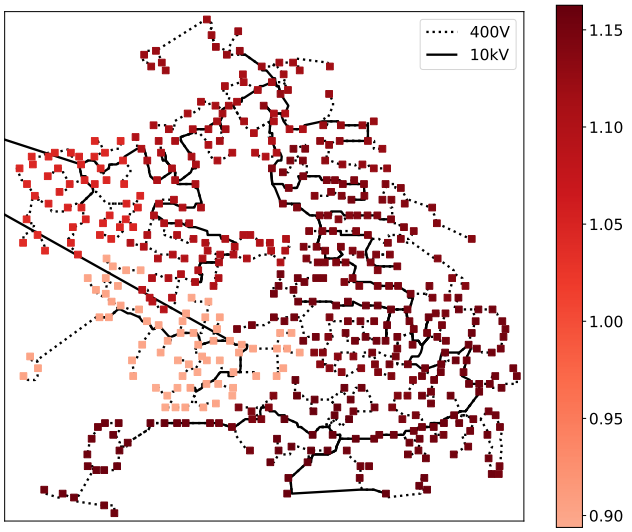

Fig. 10: Voltage

the network at this time-stamp is 2.1 MW, whereas the PV and WPP generation is 49 kW and 226 kW respectively. Fig. **??** highlights and grades distribution lines in the LV network according to the active power loss at this timestamp. The total active power loss for the network at this timestamp is 83 kW.

V. Discussion

This paper proposes and presents the development of a multi-voltage active distribution network model with a large share of weather-dependent generation, developed using a top-down approach. The foundation of the distribution network presented is a real Danish 60 kV distribution network along with measurement data for load and generation time-series for a period of about 10 months. The 60 kV network is expanded with 10 kV-400 V distribution networks generated from a publicly available Distribution Network Modeling tool (DiNeMo) [20]. Furthermore, standard load profiles (SLPs) are employed from an open-source data set called *SimBench* [22], whereas, the weather-dependent generation time-series for PV and WPPs are simulated from *CorRES* using meteorological data.

The presented results exhibit an uncategorized load profile for the presented example. This uncategorized profile is due to the mismatch between solution time-series with SLPs and weather-dependent generation and the aggregated load profile at 10 kV. The root mean square error for the optimization is an indicator of the degree of mismatch, which for the LV network at Bus-27 is about 9 % of the maximum demand at the 60 kV/10 kV substation. The root mean square error observed, while generating other LV networks, is in the range of 6 %-20 % of the absolute maximum demand at 60 kV/10 kV substation, while the correlation between the solution profile and the aggregated load time-series at 10 kV is in the range from 0.76-0.93.

One of the major sources of errors is the discrepancy in provenance of the aggregated load time-series and the standard load profiles (SLPs) used. The aggregated load time-series at 10 kV represent measurement data for a distribution network in Denmark, while the SLPs from *SimBench* are derived from distribution network measurement data in Germany. In addition, the aggregated load time-series at 10 kV are based on the year 2015, while the SLPs used for its decomposition are from the year 2016. Since, weather conditions deeply affect the load consumption behavior, the aggregated load time-series at 10 kV fails to be completely categorized using the available SLPs. Yet another major sources of mismatch are the simulated wind and photovoltaic generation profiles. Even though, the generation profiles are simulated from meteorological data for the same time-period as the aggregated load time-series at 10 kV, the simulation model in *CorRES* does not account for shut-down periods, storm-shut down, maintenance periods, etc. of the WPP and PV installations. All of the above mentioned differences in the raw-data are intractable.

However, despite the characteristic differences in the raw data, the solution presented to categorize the aggregated load time-series combined with the uncategorized load profile provides satisfactory representations of diverse generic LV networks.

Acknowledgment

This project has received funding from the European Union's Horizon 2020 research and innovation program under the Marie Sklodowska-Curie grant agreement No 861398 and Energy Technology Development and Demonstration Program (EUDP) 2019-II IEA Task 41 Journal Number 64019-0518.

References

[1] A. Peter;, "National Survey Report of PV Power Applications in Denmark," PA Energy Ltd. Denmark, Tech. Rep. August, 2016.
[2] Colin Walsh, "Wind energy in Europe in 2019," Tech. Rep., 2019.
[3] "Key World Energy Statistics 2014," Tech. Rep., 2014. [Online]. Available: www.africa-eu-renewables.org
[4] R. A. Walling, R. Saint, R. C. Dugan, J. Burke, and L. A. Kojovic, "Summary of distributed resources impact on power delivery systems," *IEEE Transactions on Power Delivery*, vol. 23, no. 3, pp. 1636–1644, 2008.
[5] K. A. Alboaouh and S. Mohagheghi, "Impact of Rooftop Photovoltaics on the Distribution System," *Journal of Renewable Energy*, vol. 2020, pp. 1–23, 2020.
[6] A. Baviskar, A. D. Hansen, K. Das, and M. Koivisto, "Challenges of Future Distribution Systems with a Large Share of Variable Renewable Energy Sources – Review," *19th Wind Integration Workshop 2020*, no. November, 2020.
[7] K. Strunz, "Developing Benchmark Models," *Symposium A Quarterly Journal In Modern Foreign Literatures*, vol. 6, no. Coll, pp. 4–5, 2005.
[8] K. Rudion, A. Orths, Z. A. Styczynski, and K. Strunz, "Design of benchmark of medium voltage distribution network for investigation of DG integration," *2006 IEEE Power Engineering Society General Meeting, PES*, p. 6 pp., 2006.
[9] K. Strunz, C. Abbey, C. Andrieu, R. C. Campbell, and R. Fletcher, *Benchmark Systems for Network Integration of Renewable and Distributed Energy Resources*, 2009, no. July.

[10] C. Canizares, T. Fernandes, E. Geraldi, L. Gerin-Lajoie, M. Gibbard, I. Hiskens Tf Past Chair, J. Kersulis, R. Kuiava, L. Lima, F. Demarco, N. Martins, B. C. Pal, A. Piardi, R. Ramos Tf Chair, J. Dos Santos, D. Silva, A. K. Singh, B. Tamimi, and D. Vowles, "Benchmark Models for the Analysis and Control of Small-Signal Oscillatory Dynamics in Power Systems," *IEEE Transactions on Power Systems*, vol. 32, no. 1, pp. 715–722, 2017.

[11] C. Matke, W. Medjroubi, and D. Kleinhans, "SciGRID - An Open Source Reference Model for the European Transmission Network (v0.2)," no. November, 2016. [Online]. Available: http://www.scigrid.de

[12] S. Coast, "Open Street Maps," 2004. [Online]. Available: www.openstreetmap.org/

[13] J. Amme, G. Pleßmann, J. Bühler, L. Hülk, E. Kötter, and P. Schwaegerl, "The eGo grid model: An open-source and open-data based synthetic medium-voltage grid model for distribution power supply systems," *Journal of Physics: Conference Series*, vol. 977, no. 1, 2018.

[14] A. Navarro-Espinosa and L. Ochoa, "Dissemination Document " Low Voltage Networks Models and Low Carbon Technology Profiles "," *Ph.D. thesis The University of Manchester*, vol. 44, no. June, pp. 1–27, 2015.

[15] D. Sarajlić and C. Rehtanz, "Low Voltage Benchmark Distribution Network Models Based on Publicly Available Data," *Proceedings of 2019 IEEE PES Innovative Smart Grid Technologies Europe, ISGT-Europe 2019*, pp. 1–5, 2019.

[16] S. Meinecke, N. Bornhorst, and M. Braun, "Power System Benchmark Generation Methodology," no. February, 2019.

[17] S. Meinecke, A. Klettke, J. Dickert, M. Hable, F. Fischer, M. Braun, A. Moser, and C. Rehtanz, "General planning and operational principles in german distribution systems used for Simbench," no. June, pp. 3–6, 2019. [Online]. Available: www.simbench.net

[18] M. Sarstedt, G. Steffen, C. Blaufus, and L. Hofmann, "Modelling of Integrated Transmission and distribution grids based on synthetic distribution grid models," *IEEE Milan Power*, 2019.

[19] K. Das, M. Altin, and A. D. Hansen, "Technical methodology for minimization of network losses," Tech. Rep. 2016, 2018.

[20] M. Grzanic, M. G. Flammini, and G. Prettico, "Distribution network model platform: A first case study," *Energies*, vol. 12, no. 21, 2019.

[21] Statistics Denmark, "Statistics Denmark," *Harvest by region, time, crop and unit*, 2013. [Online]. Available: http://www.statbank.dk/HALM1

[22] C. Spalthoff, D. Sarajlić, C. Kittl, S. Drauz, T. Kneiske, C. Rehtanz, and M. Braun, "SimBench : Open source time series of power load , storage and genera- tion for the simulation of electrical distribution grids," no. September, pp. 447–452, 2019.

[23] M. Koivisto, K. Das, F. Guo, P. Sørensen, E. Nuño, N. Cutululis, and P. Maule, "Using time series simulation tools for assessing the effects of variable renewable energy generation on power and energy systems," *Wiley Interdisciplinary Reviews: Energy and Environment*, vol. 8, no. 3, pp. 1–15, 2019.

[24] ESMAP, SOLARGIS, WB, and IFC, "Global Solar Atlas," p. 1, 2019. [Online]. Available: https://globalsolaratlas.info/?m=sg:ghi

[25] R. T. Sataloff, M. M. Johns, and K. M. Kost, "Energistyrelsen." [Online]. Available: https://ens.dk/

[26] H. Sakoe and S. Chiba, "Dynamic Programming Algorithm Optimization for Spoken Word Recognition," *IEEE Transactions on Acoustics, Speech, and Signal Processing*, vol. 26, no. 1, pp. 43–49, 1978.

[27] L. Rabiner and B.-H. Juang, *Fundamentals of speech recognition*, 1993.

[28] T. Giorgino, "Computing and visualizing dynamic time warping alignments in R: The dtw package," *Journal of Statistical Software*, vol. 31, no. 7, pp. 1–24, 2009.

[29] D. Deriso and S. Boyd, "A General Optimization Framework for Dynamic Time Warping," pp. 1–23, 2019. [Online]. Available: http://arxiv.org/abs/1905.12893